Supplementary Information for

_O_-GlcNAcylation on LATS2 disrupts the Hippo pathway by inhibiting its activity

Eunah Kim, Jeong Gu Kang, Min Jueng Kang, Jae Hyung Park, Yeon Jung Kim, Tae Hyun Kweon, Han-Woong Lee, Eek-hoon Jho, Yong-ho Lee, Seung-Il Kim, Eugene C. Yi, Hyun Woo Park, Won Ho Yang, Jin Won Cho

Corresponding author: Jin Won Cho
Email: chojw311@yonsei.ac.kr

This PDF file includes:

www.pnas.org/cgi/doi/10.1073/pnas.1913469117

Supplementary Information Text

SI Materials and Methods

Antibodies

anti-HA (Sigma, #H3663), anti-c-Myc (Santa Cruz Biotechnology, Santa Cruz, CA, USA, #sc-47694), anti-Flag (MBL, Woburn, MA, USA, #M185-3L), anti-MST1 (Abcam, Hong Kong, China, #ab76822), anti-p-T183-MST1 (Cell Signaling Technology (CST), Boston, MA, USA, #3681S), anti-LATS1(CST, #3477S), anti-LATS2 (Bethyl Laboratories Inc., Montgomery, AL, USA, #A300-479A or Abnova, Taipei, Taiwan, #MAB0019 or Proteintech Group, Chicago, IL, USA, #20276-1-AP), anti-p-hydrophobic motif-LATS (CST, #8654), anti-p-activation loop-LATS (CST, #9157), anti-YAP (Santa Cruz Biotechnology, #sc-15407 or Abnova, #H00010413-M01 or CST, #14074), anti-p-S127-YAP (CST, #4911), anti-p-S109-YAP (CST, #46931), anti-TAZ (CST, #4883 or BD pharmigen, BD PharMingen, San Diego, CA, USA, #560235), anti-p-S89-TAZ (CST, #59971), anti-*O*-GlcNAc (CTD110.6: Covance, Princeton, NJ, USA, #MMS-248R or RL2: Thermo Fisher Scientific, #MA1-072), anti-OGT (Sigma, #O6264), anti-CTGF (Santa Cruz Biotechnology, #sc-365970 or #sc-14939), anti-CYR61 (Santa Cruz Biotechnology, #sc-374129 or sc-13100), anti-RHAMM (Santa Cruz Biotechnology, #sc-515221), anti-ERK2 (Santa Cruz Biotechnology, #sc-1647), anti-phospho-ERK1 ($pThr^{202}/pTyr^{204}$) and ERK2 ($pThr^{185}/pTyr^{187}$) (Sigma, #E7028), anti-β-actin (CST, #4970), anti-α-tubulin (Santa Cruz Biotechnology, #sc-8035), anti-lamin A/C (CST, #2032), and anti-GAPDH (Santa Cruz Biotechnology, #sc-32233 or Millipore, Burlington, MA, USA, #M171-3). The results acquired by Western blotting were quantified using Multi Gauge Ver 3.1 software (Fuji Film Corp., Tokyo, Japan).

siRNA sequences

siOGT sense: 5′-UAAUCAUUUCAAUAACUGCUUCUGC (dTdT)-3′,
siOGT antisense: 5′-GCAGAAGCAGUUAUUGAAA UGAUUA (dTdT)-3′.
siLATS2 sense: 5-′CACACACACACACAGAGAU (dTdT)-3′
siLATS2 antisense:5′-AUCUCUGUGUGUGUGUG (dTdT)-3′

Quantitative RT-PCR primer sequences

CTGF, forward 5′-GTTTGGCCCAGACCCAACT-3′
CTGF, reverse 5′-GGAACAGGCGCTCCACTCT-3′
CYR61, forward 5′-AGCCTCGCATCCTATACAAC-3′
CYR61, reverse 5′-TTCTTTCACAAGGCGGCATC-3′
RHAMM, forward 5′-AGAACCAACTCAAGCAACAGG-3′
RHAMM, reverse 5′-AGGAGACGCCACTTGTTAATTTC-3′
LATS2, forward 5′-GTAGGACGCAAACGAAT-3′
LATS2, reverse 5′-CAGAAGTGAACCGGCA-3’
NF2, forward 5′-AGCTTCAACCTCATTGGTGACAGC-3′
NF2, reverse 5′-TGAGTTCATTGAGCTGCTCCTGC-3′
GAPDH, forward 5′-AGGGCTGCTTTTAACTCTGGT-3′
GAPDH, reverse 5′-CCCCACTTGATTTTGGAGGGA-3′

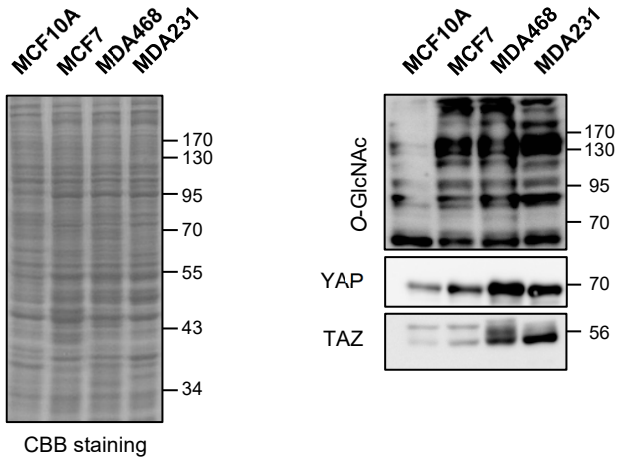

Fig. S1. Cellular *O*-GlcNAcylation and YAP/TAZ expression level in breast cancer cells are higher than those in normal breast cells. Normal breast cells (MCF10A) and three breast cancer cell lines (MCF7, MDA-MB-468, and MDA-MB-231) were incubated for 3 days. Their respective cell lysates were stained with Coomassie Blue G250 and immunoblotted with the relevant antibodies. A CBB-stained gel was used as a loading control.

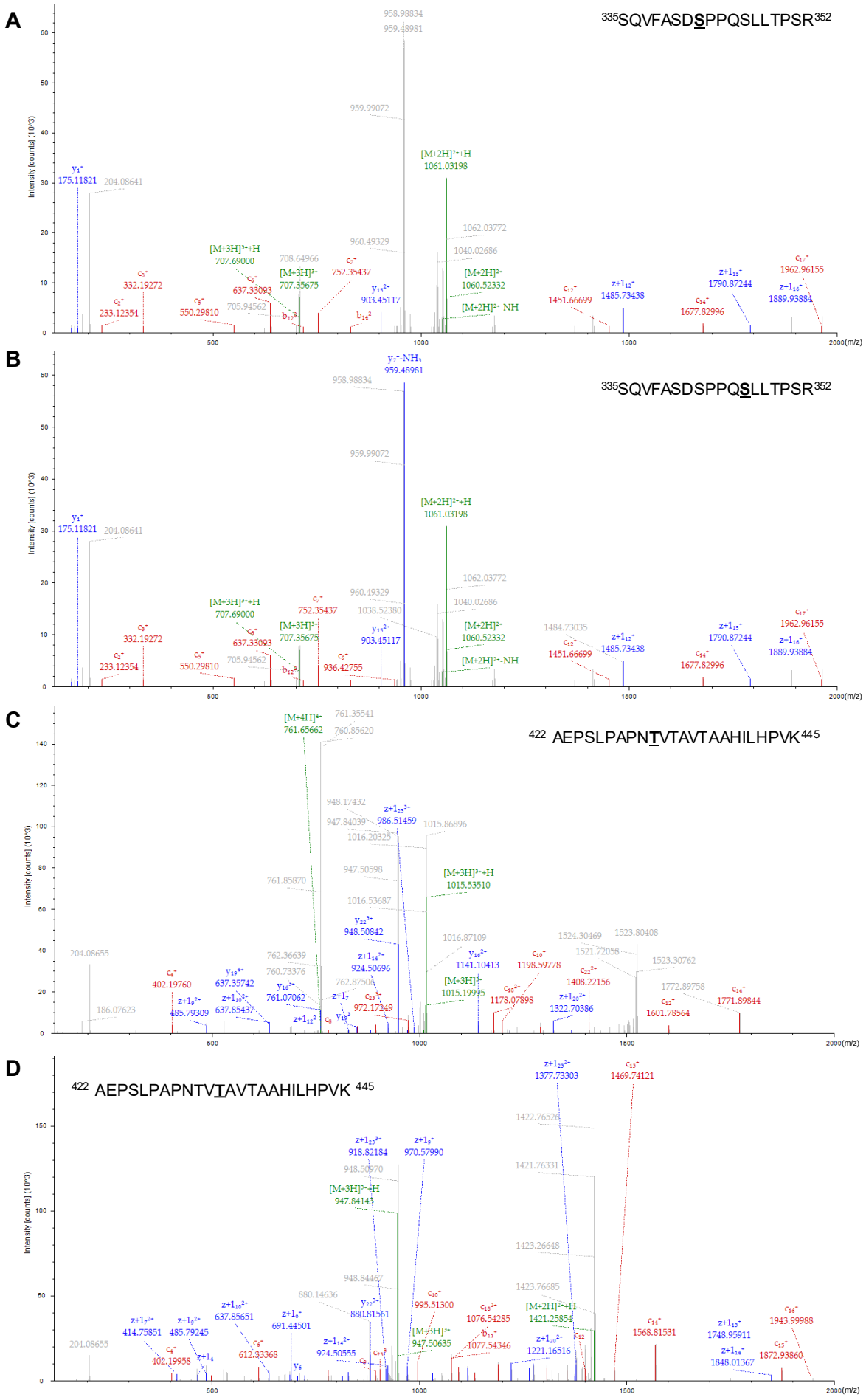
A
335SQVFASDSPPQSLLTPSR352
B
335SQVFASDSPPQSLLTPSR352
C
422 AEPSLPAPNTVTAVTAAHILHPVK445
D
422 AEPSLPAPNTVTAVTAAHILHPVK 445
Intensity [counts] (10^3)
m/z

Fig. S2. Mass spectrometry analysis reveals the minor LATS2 *O*-GlcNAc sites. *(A) O*-GlcNAcylation was detected at LATS2 Ser342. This peptide corresponds to residues 335–352, SQVFASDSPPQSLLTPSR. Ser342 is bolded and underlined in the sequence. The *O*-GlcNAc oxonium ions (m/z, 204.09, 186.08) were also assigned. *(B) O*-GlcNAcylation was detected at LATS2 Ser346. This peptide corresponds to residues 335–352, SQVFASDSPPQSLLTPSR. Ser346 is bolded and underlined in the sequence. The *O*-GlcNAc oxonium ions (m/z, 204.09, 186.08) were also assigned. *(C) O*-GlcNAcylation was detected at LATS2 Thr431. This peptide corresponds to residues 422–445, AEPSLPAPNTVTAVTAAHILHPVK. Thr431 is bolded and underlined. The *O*-GlcNAc oxonium ions (m/z, 204.09, 186.08) were also assigned. *(D) O*-GlcNAcylation was detected at LATS2 Thr433. This peptide corresponds to residues 422–445, AEPSLPAPNTV TAVTAAHILHPVK. Thr433 is bolded and underlined in the sequence. The *O*-GlcNAc oxonium ions (m/z, 204.09, 186.08) were also assigned

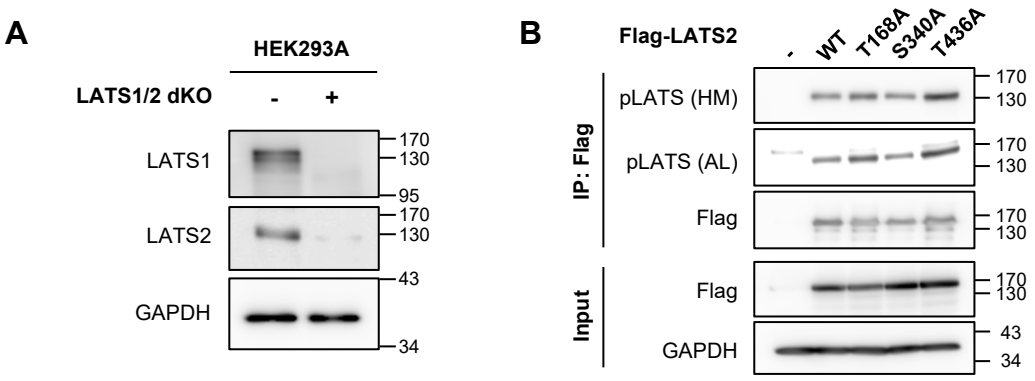

Fig. S3. LATS2 *O*-GlcNAcylation inhibits its phosphorylation in LATS1/2-dKO HEK293A cells. (A) LATS1/2 are knocked out in LATS1/2-dKO HEK293A cells. (B) Flag-tagged wild-type LATS2 or LATS2 mutants was stably expressed in LATS1/2-dKO HEK293A cells, and immunoprecipitated Flag-LATS2 was detected with phospho-specific LATS antibodies. Abbreviations: HM (hydrophobic motif), AL (Activation loop)

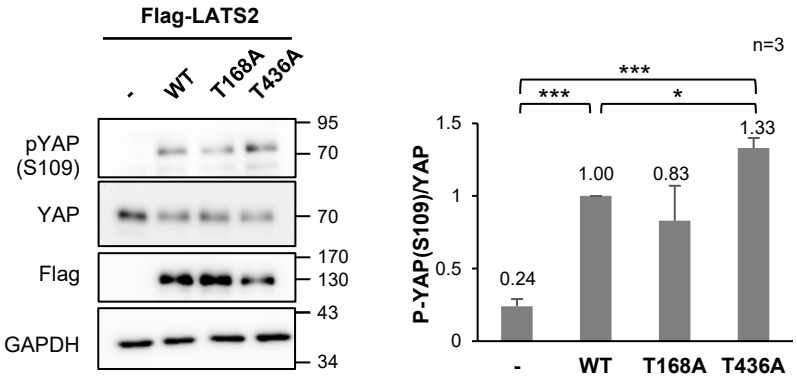

Fig. S4. Lack of *O*-GlcNAcylation at LATS2 Thr436 increased phosphorylation at YAP Ser109. Wild-type LATS2 or LATS2 mutants were stably expressed in LATS1/2-dKO HEK293A cells. Phosphorylation at YAP Ser109 was detected by anti-p-S109-YAP antibody. The phosphorylation level at YAP Ser109 was normalized to total YAP level. Data are presented as mean ± SEM from three independent experiments. Statistical significance was determined by one-way ANOVA (*$p < 0.05$, ***$p < 0.005$).

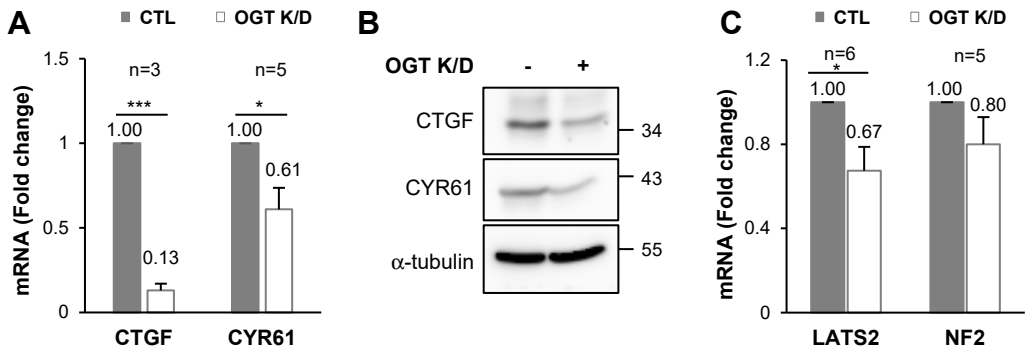

Fig. S5. Transcription and expression levels of CTGF and CYR61 decreased upon OGT knockdown, and mRNA levels of LATS2 and NF2 also decreased. *(A–C)* MDA-MB-231 cells were transfected with OGT siRNA for 48 h. *(A)* Relative mRNA levels of CTGF and CYR61 in MDA-MB-231 cells were determined by quantitative real-time PCR. All values were normalized to the GAPDH mRNA level. *(B)* CTGF and CYR61 levels were determined by immunoblotting. *(C)* Relative mRNA levels of NF2 and LATS2 were determined by quantitative real-time PCR. All values were normalized to GAPDH mRNA level. *(A, C)* Data are presented as mean ± SEM from at least three independent experiments. Differences were detected by the two-tailed Student's *t*-test (*$p < 0.05$, ***$p < 0.005$).

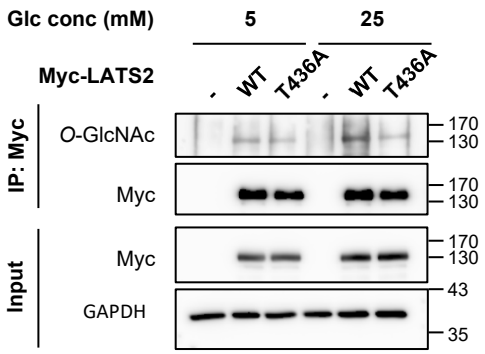

Fig. S6. LATS2 *O*-GlcNAcylation at Thr436 is affected by extracellular glucose status. MDA-MB-231 cells transfected with wild-type or T436A mutant LATS2 were grown in 5 mM or 25 mM glucose containing media. Each immunoprecipitated LATS2 wild-type and T436A mutant was immunoblotted with anti-*O*-GlcNAc antibody.

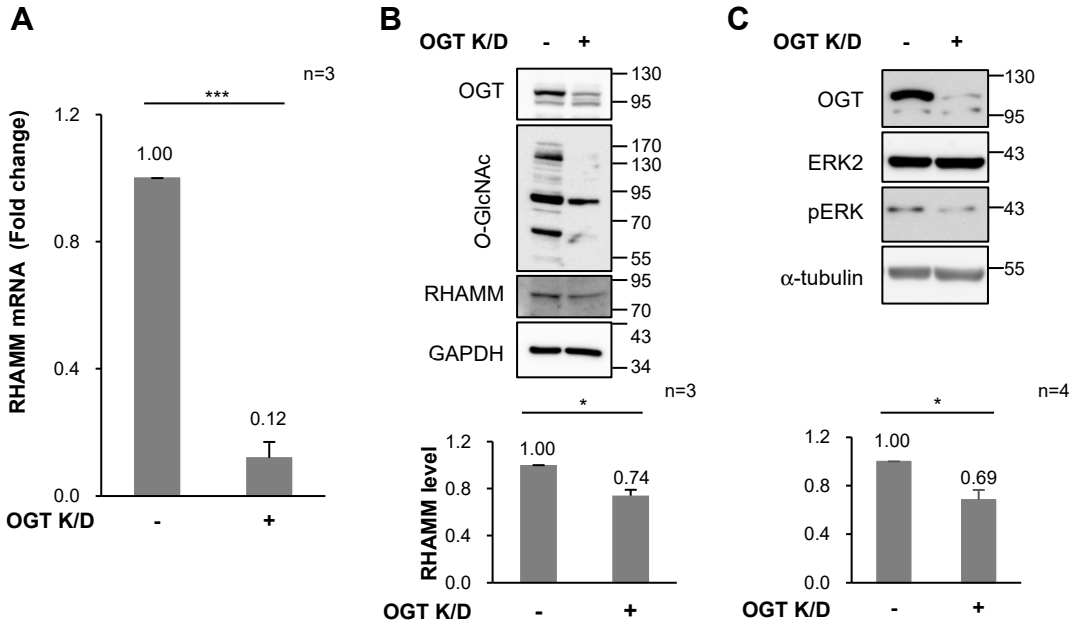

Fig. S7. A decrease in global *O*-GlcNAcylation reduced RHAMM and phosphorylation of ERK in MDA-MB-231 cells. *(A–C)* MDA-MB-231 cells were transfected with OGT siRNA for 48 h. *(A)* The relative RHAMM mRNA level was determined by qRT-PCR. The RHAMM mRNA level was normalized to that of GAPDH. *(B,C)* Respective cell lysates were immunoblotted with the relevant antibodies. The amount of RHAMM was normalized to that of GAPDH *(B)* and the phosphorylation level of ERK was normalized to that of ERK2 *(C)*. *(A–C)* Data are presented as mean ± SEM from at least three independent experiments. Statistical significance was determined by the two-tailed Student's *t*-test (*$p < 0.05$, ***$p < 0.005$).